

Synthesis of the Water Soluble Ligands dmPTA and dmoPTA and the Complex [RuClCp(HdmoPTA)(PPh₃)](OSO₂CF₃) (dmPTA = *N,N*-Dimethyl-1,3,5-triaza-7-phosphaadamantane, dmoPTA = 3,7-Dimethyl-1,3,7-triaza-5-phosphabicyclo[3.3.1]nonane, HdmoPTA = 3,7-H-3,7-Dimethyl-1,3,7-triaza-5-phosphabicyclo[3.3.1]nonane)

Adrián Mena-Cruz,[‡] Pablo Lorenzo-Luis,[‡] Antonio Romerosa,^{*†} Mustapha Saoud,[†] and Manuel Serrano-Ruiz[†]

Area de Química Inorgánica, Facultad de Ciencias, Universidad de Almería, Almería, Spain, and Departamento de Química Inorgánica, Facultad de Química, Universidad de La Laguna, La Laguna, Tenerife, Spain

Received January 30, 2007

The new water-soluble ligand dmPTA(OSO₂CF₃)₂ (**1**) (dmPTA = *N,N*-dimethyl-1,3,5-triaza-7-phosphaadamantane) has been synthesized by reaction of PTA with MeOSO₂CF₃ in acetone (PTA = 1,3,5-triaza-7-phosphatricyclo[3.3.1.1^{3,7}]decane). The reaction of **1** with KOH gave rise to the new water-soluble ligand dmoPTA (**3**) (dmoPTA = 3,7-dimethyl-1,3,7-triaza-5-phosphabicyclo[3.3.1]nonane) by elimination of the –CH₂– group located between both NCH₃ units. Compound dmPTA(BF₄)₂ (**2**) and complex [RuClCp(HdmoPTA)(PPh₃)](OSO₂CF₃) (**4**) have also been synthesized, while compounds HdmoPTA(BF₄) (**3a**) and [RuClCp(dmPTA)(PPh₃)](OSO₂CF₃) (**5**) were characterized but not isolated. The new ligands and the complex have been fully characterized by NMR, IR, elemental analysis, and X-ray crystal structure determination (ligand **1** and complex **4**). The synthetic processes for **3** and **4** were studied.

Introduction

Water is the ideal solvent for synthetic processes from an economical and ecological industrial point of view. As a consequence, aqueous organometallic chemistry has received much attention in recent years.^{1–8} Water-soluble metal complexes able to catalyze the synthetic processes in water

are mandatory. Tertiary water-soluble phosphines have been the most widely used class of aqua-soluble ligands for catalysis in water because of their neutral donating ability that can effectively stabilize the metal center throughout several catalytic cycles. Varieties of aqua-soluble phosphines have appeared through the years, and their catalytic potential has been investigated. Our research group has paid special attention to the air-stable and economical to obtain ligand 1,3,5-triaza-7-phosphaadamantane (PTA) and its *N*-methyl derivative *N*-methyl-1,3,5-triaza-7-phosphaadamantane (mPTA).^{9–11} These ligands have been shown to react with metals to give rise to water-soluble complexes with new interesting properties. Recently, we have published the

* To whom correspondence should be addressed. E-mail: romerosa@ual.es.

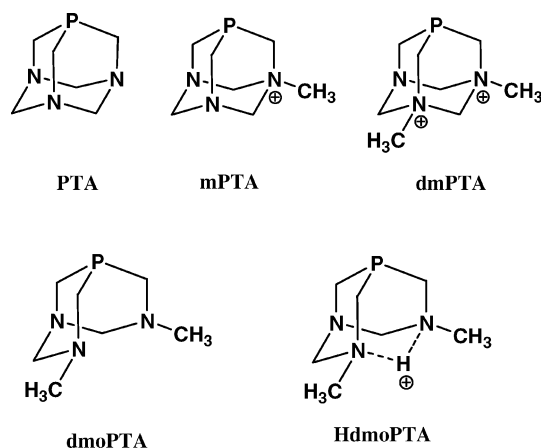
[†] Universidad de Almería.

[‡] Universidad de La Laguna, La Laguna.

- (1) Joó, F. *Aqueous Organometallic Catalysis*; Kluwer: Dordrecht, The Netherlands, 2001.
- (2) Cornils, B.; Herrmann, W. A., Eds. *Aqueous-Phase Organometallic Catalysis. Concepts and Applications*; Wiley-VCH: Weinheim, Germany, 1998.
- (3) Horváth, I. T.; Joó, F., Eds. *Aqueous Organometallic Chemistry and Catalysis*; NATO ASI 3/5; Kluwer: Dordrecht, The Netherlands, 1995.
- (4) Sinou, D. *Top. Curr. Chem.* **1999**, *206*, 41.
- (5) (a) Frost, B. J.; Mebi, C. A. *Organometallics* **2004**, *23*, 5317. (b) Darensbourg, D. J.; Ortiz, C. G.; Kamplain, J. W. *Organometallics* **2004**, *23*, 1747. (c) Darensbourg, D. J.; Joó, F.; Kannisto, M.; Kathó, A.; Reibenspies, J. H.; Daigle, D. J. *Inorg. Chem.* **1994**, *33*, 200.
- (6) Phillips, A. D.; Gonsalvi, L.; Romerosa, A.; Vizza, F.; Peruzzini, M. *Coord. Chem. Rev.* **2004**, *248*, 955.
- (7) Mohr, F.; Cerrada, E.; Laguna, M. *Organometallics* **2006**, *25*, 644.

- (8) Mohr, F.; Sanz, S.; Tiekink, E. R. T.; Laguna, M. *Organometallics* **2006**, *25*, 3084.
- (9) Akbayeva, D. N.; Gonsalvi, L.; Oberhauser, W.; Peruzzini, M.; Vizza, F.; Brüggeller, P.; Romerosa, A.; Sava, G.; Bergamo, A. *Chem. Commun.* **2003**, 264.
- (10) Lidrissi, C.; Romerosa, A.; Saoud, M.; Serrano-Ruiz, M.; Gonsalvi, L.; Peruzzini, M. *Angew. Chem., Int. Ed.* **2005**, *44*, 2568.
- (11) Romerosa, A.; Campos-Malpartida, T.; Lidrissi, C.; Saoud, M.; Serrano-Ruiz, M.; Peruzzini, M.; Garrido-Cárdenas, J. A.; García-Maroto, F. *Inorg. Chem.* **2006**, *45*, 1289.

Chart 1



synthesis of the piano-stool complexes $[\text{RuCpX}(\text{L})(\text{L}')]^{n+}$ ($\text{X} = \text{Cl}, \text{I}$; $\text{L} = \text{PPh}_3$; $\text{L}' = \text{PTA}, \text{mPTA}$; $\text{L} = \text{L}' = \text{PTA}, \text{mPTA}$) that display a tuned DNA activity depending on the water-soluble phosphine coordinated to the metal. Therefore, an accurate selection of ligands could provide ruthenium complexes with tuned DNA activity.

Although other derivatives of PTA have also been synthesized, but they remain relatively unexplored because their metal complexes are not water soluble.^{12–15} The synthesis of new water-soluble phosphines to serve as ligands to lower valence metal complexes rendering them soluble in water is required. We have investigated the synthesis and coordination properties of 1,3-dimethyl-1,3-bis-(azonia)-5-aza-7-phosphatricyclo[3.3.1.1^{3,7}]decane (dmPTA) (Chart 1). This dicationic ligand has a similar ligand angle and electronic properties but has a water solubility greater than that of PTA.

Herein, we report complete characterization of the new water-soluble ligand dmPTA and its reaction with $[\text{RuClCp}(\text{PPh}_3)_2]$. As a consequence, the unexpected complex $[\text{RuClCp}(\text{HdmoPTA})(\text{PPh}_3)](\text{OSO}_2\text{CF}_3)$ (**4**) was obtained. In this complex, the ligand bonded to the metal is not the starting phosphine dmPTA but a new one, the 3,7-H-3,7-dimethyl-1,3,7-triaza-5-phosphabicyclo[3.3.1]nonane (HdmoPTA) (Chart 1). In addition, we have studied the process for formation of complex **4**.

Experimental Section

General Procedures. All chemicals were reagent grade and, unless otherwise stated, were used as received by commercial suppliers. Likewise all reactions were carried out in a pure argon atmosphere using standard Schlenk-tube techniques with freshly distilled and oxygen-free solvents. The hydrosoluble phosphine PTA and complex $[\text{RuClCp}(\text{PPh}_3)_2]$ were prepared as described in the literature.^{9,11} ^1H and $^{13}\text{C}\{^1\text{H}\}$ NMR spectra were recorded on a Bruker DRX300 spectrometer operating at 300.13 (^1H) and

75.47 MHz (^{13}C), respectively. Peak positions are relative to tetramethylsilane and were calibrated against the residual solvent resonance (^1H) or the deuterated solvent multiplet (^{13}C). $^{31}\text{P}\{^1\text{H}\}$ and $^{19}\text{F}\{^1\text{H}\}$ NMR spectra were recorded on the same instrument operating at 121.49 and 282.40 MHz, respectively. Chemical shifts for $^{31}\text{P}\{^1\text{H}\}$ NMR were measured relative to external 85% H_3PO_4 , and for $^{19}\text{F}\{^1\text{H}\}$ NMR to CFCl_3 , they were measured with downfield values taken as positive in both cases. All NMR spectra were obtained at 25 °C. Infrared spectra were recorded as KBr disks using a Thermo Nicolet Avatar 360 FT-IR spectrometer. Elemental analyses (C, H, N, S) were performed on a Fisons Instrument EA 1108 elemental analyzer.

Synthesis of dmPTA(OSO_2CF_3)₂ (1**).** $\text{CH}_3\text{OSO}_2\text{CF}_3$ (0.180 mL, 1.60 mmol) was added via a syringe to a vigorously stirred solution of PTA (250 mg, 1.60 mmol) in 50 mL of acetone at 45 °C. After 20 min, an additional 0.180 mL of $\text{CH}_3\text{OSO}_2\text{CF}_3$ was added, and then the solution was refluxed for 2 h, after which the solvent was evaporated to ~90%. The addition of CHCl_3 (5 mL) and the cooling of the mixture at 0 °C produced an abundant white precipitate, which was stirred for 30 min, filtered, washed with cold ether/acetone (2.5/1 mL), and vacuum-dried.

A solution of **1** (50 mg, 0.10 mmol) in commercial acetone (7.5 mL) was evaporated at room temperature. From the filtrate, prismatic colorless crystals suitable for X-ray diffraction were collected after several days.

Yield: 0.40 g, 52%. $S_{25^\circ\text{C}, \text{H}_2\text{O}} = 12$ mg/mL. Elemental analysis for powder sample $\text{C}_{10}\text{H}_{18}\text{N}_3\text{F}_6\text{O}_6\text{P}_1\text{S}_2$ (485.36 g mol⁻¹): found C 24.80, H 4.08, N 8.08, 12.26; calcd C 24.72, H 3.71, N 8.65, S 13.19%. Elemental analysis for crystal sample $\text{C}_{10}\text{H}_{20}\text{N}_3\text{F}_6\text{O}_7\text{P}_1\text{S}_2$ (503.36 g mol⁻¹): found C 24.75, H 4.02, N 8.03, S 12.37%; calcd C 24.81, H 3.97, N 8.34, S 12.71%. IR (KBr, cm⁻¹): $\nu_{(\text{OTf})}$ 1274, 1252, 1170, 1158. ^1H NMR (DMSO-*d*₆): δ 3.03 (s, NCH_3 , 6 H), 3.78 (d, $^2J_{\text{HP}} = 11.55$ Hz, PCH_2N , 2 H), 4.25–4.71 (m, PCH_2NCH_3 , 4 H), 4.87–5.46 (m, NCH_2N , 6 H). ^1H NMR (acetone-*d*₆): δ 3.40 (s, NCH_3 , 6 H), 4.12 (d, $^2J_{\text{HP}} = 11.97$ Hz, PCH_2N , 2 H), 4.62–5.13 (m, PCH_2NCH_3 , 4 H), 5.19–5.69 (m, NCH_2N , 6 H). ^1H NMR (D_2O): δ 3.16 (s, NCH_3 , 6 H), 3.85 (d, $^2J_{\text{HP}} = 12.30$ Hz, PCH_2N , 2 H), 4.27–4.63 (m, PCH_2NCH_3 , 4 H), 4.92–5.21 (m, NCH_2N , 6 H). $^{13}\text{C}\{^1\text{H}\}$ NMR (DMSO-*d*₆): δ 42.53 (d, $^1J_{\text{CP}} = 21.09$ Hz, PCH_2N), 52.12 (s, CH_3), 54.29 (d, $^1J_{\text{CP}} = 32.47$ Hz, PCH_2NCH_3), 77.55 (s, $\text{CH}_3\text{NCH}_2\text{NCH}_3$), 78.26 (s, NCH_2NCH_3), 119.82 (q, $^1J_{\text{CF}} = 316.21$ Hz, OTf). $^{13}\text{C}\{^1\text{H}\}$ NMR (acetone-*d*₆): δ 42.17 (d, $^1J_{\text{CP}} = 21.80$ Hz, PCH_2N), 51.65 (s, CH_3), 54.45 (d, $^1J_{\text{CP}} = 38.50$ Hz, PCH_2NCH_3), 77.74 (s, $\text{CH}_3\text{NCH}_2\text{NCH}_3$), 78.68 (s, NCH_2NCH_3), 120.78 (q, $^1J_{\text{CF}} = 320.00$ Hz, OTf). $^{31}\text{P}\{^1\text{H}\}$ NMR (DMSO-*d*₆): δ -81.71 (s). $^{31}\text{P}\{^1\text{H}\}$ NMR (acetone-*d*₆): δ -79.68 (s). $^{31}\text{P}\{^1\text{H}\}$ NMR (D_2O): δ -80.78 (s).

Synthesis of dmPTA(BF_4)₂ (2**).** Forty-six milligrams of NaBF_4 (0.42 mmol) was added to a solution containing 100 mg of **1** (0.21 mmol) in 25 mL of acetone at 45 °C. A white powder slowly separated and was filtered out after 2 h, washed with acetone (2 × 2 mL), and air-dried.

Yield: 0.047 g, 62%. $S_{25^\circ\text{C}, \text{H}_2\text{O}} = 8.4$ mg/mL. Elemental analysis for $\text{C}_8\text{H}_{18}\text{N}_3\text{F}_8\text{P}_1$ (339.21 g/mol): found C 27.96, H 5.45, N 11.87; calcd C 28.30, H 5.30, N 12.38. IR (KBr, cm⁻¹): $\nu_{(\text{BF}_4)}$ 1107, 1080, 1052.

Synthesis of dmoPTA (3**).** Compound **3** was prepared through two alternative processes.

(A) The reaction of 200 mg of dmPTA(OSO_2CF_3)₂ (**1**) (0.412 mmol) with 16.5 mg of KOH (0.412 mmol) in 20 mL of water led to a colorless solution, which was stirred for 30 min at room temperature and then concentrated to 1 mL. The addition of 5 mL of acetone and 5 mL of Et_2O gave rise to a white powder, which

- (12) Frost, B. J.; Bautista, C. M.; Huang, R.; Shearer, J. *Inorg. Chem.* **2006**, *45*, 3481.
 (13) Frost, B. J.; Mebi, C. A.; Gingrich, P. W. *Eur. J. Inorg. Chem.* **2006**, 1182.
 (14) Mohr, F.; Falvello, L. R.; Laguna, M. *Eur. J. Inorg. Chem.* **2006**, 3152.
 (15) Darensbourg, D. J.; Yarbrough, J. C.; Lewis, S. J. *Organometallics* **2003**, *22*, 2050.

was filtered out and washed with Et₂O (2 × 2 mL). The preferred compound was obtained by evaporation of the filtered solution and by washing with water.

(B) KOH (27.2 mg, 0.412 mmol) and dmPTA(OSO₂CF₃)₂ (**1**) (200 mg, 0.412 mmol) were dissolved in 20 mL of MeOH. After the mixture was refluxed for 1 h, the resulting colorless solution was evaporated to 2 mL, and then 5 mL of Et₂O was added. The resulting white precipitate was filtered and washed with Et₂O (2 × 2 mL). The filtered solution and filtered Et₂O were combined and evaporated to obtain a white powder.

Yield: (A) 0.046 g, 65%; (B) 0.039 g, 55%. S_{25°C}, H₂O = 42 mg/mL. Elemental analysis for powder sample C₇H₁₆N₃ (142.22 g mol⁻¹): found C 58.92, H 11.37, N 29.13; calcd C 59.06, H 11.25; N 29.53. ¹H NMR (D₂O): δ 2.37 (s, NCH₃, 6 H), 3.32–3.73 (brm, PCH₂NCH₃, 4 H), 3.38 (d, ²J_{HP} = 11.01 Hz, PCH₂N, 2 H), 3.96–4.28 (brm, NCH₂NCH₃, 4 H). ¹³C{¹H} NMR (D₂O): δ 42.56 (d, ¹J_{CP} = 16.30 Hz, PCH₂N), 43.02 (s, CH₃) 51.18 (d, ¹J_{CP} = 25.24 Hz, PCH₂NCH₃), 75.30 (s, NCH₂NCH₃). ³¹P{¹H} NMR (D₂O): δ -70.72 (s).

Reactivity of 1 with HBF₄·Et₂O and KOH. Both of the following reactions were performed by a similar procedure. Compound **1** (15 mg, 0.03 mmol) was dissolved in 0.5 mL of D₂O in a 5 mm NMR tube, and then (a) HBF₄·Et₂O (3.8 μL mg, 0.03 mmol) and (b) KOH (2 mg, 0.03 mmol) were added.

The ³¹P{¹H} NMR spectra obtained at different times for reaction a did not show any significant change. For reaction b, the starting compound transformed to give the ligand dmoPTA (**3**) quantitatively after 2 h, which remained stable in solution for 24 h at room temperature. The ¹H and ¹³C{¹H} NMR for reaction b showed singlets at 4.72 and 81.76 ppm, respectively, in addition to the signals ascribable to **3**. By evaporation of the solvent, a white powder was obtained that was freshly dissolved in D₂O. The NMR spectra of the resulting solution showed only signals for **3**. Signals at 4.72 ppm (¹H NMR) and 81.76 ppm (¹³C{¹H} NMR) were newly observed by addition into the solution of 1 μL of CH₂O. Finally, if the reaction was performed only using 0.8 equiv of KOH, compound **3** and CH₂O were obtained in yield of ~80%.

Reactivity of 3 with HBF₄. Synthesis of HdmoPTA(BF₄) (3a). Compound **3** (15 mg, 0.09 mmol) was dissolved in a 5 mm NMR tube containing 0.5 mL of D₂O and 1 equiv of HBF₄·Et₂O (10.5 μL, 0.09 mmol). The ³¹P{¹H} NMR showed the immediate and quantitative transformation to a new compound which was not stable in solution long enough for a full spectroscopic characterization. Prior to decomposition, 1 equiv of KOH was introduced into the NMR tube (4.86 mg, 0.09 mmol) that led to the starting compound **3**. By a similar procedure, **3** was reacted with 0.5, 0.9, and 1.2 mmol of HBF₄·Et₂O that led to 50, 90, and 100%, respectively, of **3a**. ¹H NMR (D₂O): δ 3.58 (s, NCH₃, 6 H), 2.84–3.22 (m, PCH₂NCH₃, 4 H), 3.83, 4.29 (m, PCH₂N, 2 H), 4.48–5.62 (brm, NCH₂NCH₃, 4 H). ³¹P{¹H} NMR (D₂O): δ -80.52 (s).

Synthesis of [RuClCp(HdmoPTA)(PPh₃)](OSO₂CF₃) (4**).** The synthesis of **4** was accomplished by employing three different methodologies.

(A) Compound **1** (0.067 g, 0.14 mmol) was added to a solution of [RuClCp(PPh₃)₂] (0.1 g, 0.14 mmol) in 10 mL of acetone. The resulting mixture was refluxed for 6 h, and the resulting yellow-orange solution was evaporated to 5 mL and cooled to 8 °C. The pale-orange precipitate obtained was filtered, washed with cool acetone (2 × 1 mL), and dried by air. Yellow-orange crystals adequate for X-ray diffraction were obtained by recrystallization from MeOH/H₂O (10:1).

(B) The solution obtained by method A was fully evaporated, and the resulting yellow powder was dissolved in 10 mL of MeOH/

H₂O (9:1). The obtained suspension was kept at reflux for 2 h, cooled, and evaporated to 2 mL. The addition of 5 mL of Et₂O led to a yellow precipitate, which was filtered out, washed with MeOH (1 × 1 mL), Et₂O (2 × 2 mL), and vacuum-dried.

(C) A yellow solution was obtained by the reaction of 50 mg of dmoPTA(CF₃SO₃) (**3**) (0.28 mmol) with 209 mg of [RuClCp(PPh₃)₂] (0.29 mmol) in 20 mL acetone. After a 2 h reflux, the solution volume was reduced to 2 mL, and 5 mL of EtOH was added to afford a yellow precipitate, which was filtered, washed with Et₂O (2 × 2 mL), and vacuum-dried.

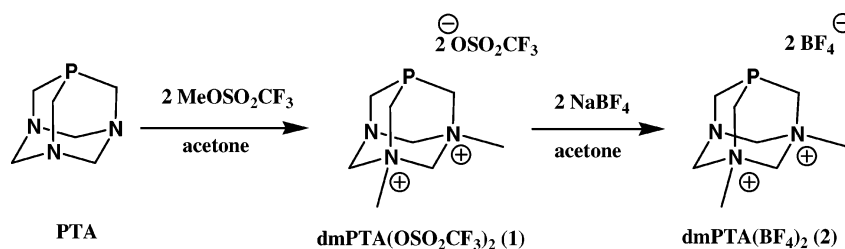
Yield: (A) 0.022 g, 20%; (B) 0.078 g, 72%; (C) 0.140 g, 62%. S_{25°C}, H₂O = 1.7 mg/mL. Elemental analysis for powder sample C₃₁H₃₇N₃P₂F₃SO₃RuCl (787.17 g mol⁻¹): found C 47.10, H 4.82, N 5.11, S 3.88; calcd C 47.26, H 4.70, N 5.33, S 4.06%. Elemental analysis for crystal sample C₃₂H₄₁N₃P₂F₃SO₄RuCl (819.22 g mol⁻¹): found C 46.54, H 4.95, N 5.21, S 3.78%; calcd C 46.87, H 5.00, N 5.13, S 3.91%. IR (KBr, cm⁻¹): ν_(OTf) 1254, 1273. ¹H NMR (CD₃OD): δ 2.38, 2.43 (s + s, NCH₃, 3 H + 3 H), 3.02–3.13 (m, PCH₂N, 2 H), 3.24–3.88 (m, PCH₂NCH₃, 4 H), 4.23–5.35 (m, NCH₂N, 4 H), 4.54 (s, Cp, 5H), 7.44–7.92 (m, aromatic, PPh₃, 15 H). ¹H NMR (acetone-*d*₆): δ 2.49 (bs, NCH₃, 6 H), 3.07–3.65 (brm, PCH₂N, 6 H), 4.02–5.68 (brm, NCH₂N, 4 H), 4.56 (s, Cp, 5H), 7.45–8.03 (m, aromatic, PPh₃, 15 H). ¹³C{¹H} NMR (CD₃-OD): δ 41.86, 41.92 (s + s, CH₃N), 47.60 (bd, ¹J_{CP} = 27.6 Hz, PCH₂N), 55.23, 56.37 (d + d, ¹J_{CP} = 12.6 Hz, ¹J_{CP} = 13.8 Hz, PCH₂NCH₃), 75.38 (s, NCH₂NCH₃), 79.30 (s, Cp), 121.02 (q, ¹J_{CF} = 312.1 Hz, CF₃SO₃⁻), 127.75–133.84 (m, aromatic, PPh₃). ¹³C{¹H} NMR (acetone-*d*₆): δ 42.32, 42.24 (s + s, CH₃N), 47.26 (bd, ¹J_{CP} = 19.8 Hz, PCH₂N), 55.30, 55.54 (bd + bd, PCH₂NCH₃), 75.36 (bs, NCH₂NCH₃), 79.56 (s, Cp), 120.42 (q, ¹J_{CF} = 314.1 Hz, CF₃SO₃⁻), 127.89–138.45 (m, aromatic, PPh₃). ³¹P{¹H} NMR (CD₃OD): δ -2.93 (d, ²J_{PP} = 42.72 Hz, HdmoPTA), 46.00 (d, ²J_{PP} = 42.72 Hz, PPh₃). ³¹P{¹H} NMR (acetone-*d*₆): δ -1.80 (bs, HdmoPTA), 46.13 (bs, PPh₃). ¹⁹F NMR (CD₃OD): δ -78.94 (s). ¹⁹F NMR (acetone-*d*₆): δ -78.86 (s).

Reactivity of 1 with [RuClCp(PPh₃)₂] in Acetone-*d*₆, D₂O, and CD₃OD. Synthesis of [RuClCp(dmPTA)(PPh₃)₂] (5**).** A 5 mm NMR tube was charged with **1** (15 mg, 0.03 mmol), [RuClCp(PPh₃)₂] (25 mg, 0.03 mmol), and 0.5 mL of dry acetone-*d*₆ using a general procedure. The resulting solution was kept at 50 °C and analyzed every 20 min by NMR. Three experiments were conducted: (a) without H₂O, (b) containing 10 μL (0.55 mmol) of H₂O, and (c) with 17 μL (0.55 mmol) of CH₃OH. From experiment a, the main complex obtained was **5**, which could not be isolated but was characterized in solution by NMR. From b and c, complex **4** was the main specie synthesized (80%). The conversion kinetic of b was larger than that of c.

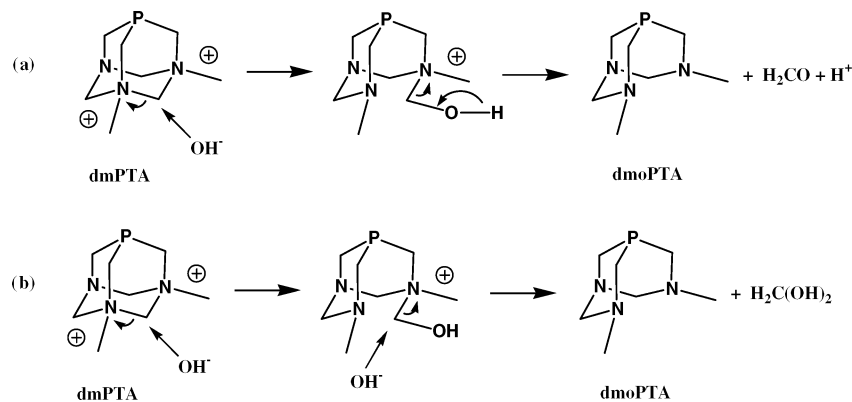
¹H NMR (acetone-*d*₆): δ 3.29 (bs, NCH₃, 6 H), 3.98 (bd, ²J_{HP} = 13.1 Hz, PCH₂N, 2 H), 4.33–5.55 (m, PCH₂NCH₃ + NCH₂N, 6 H), 4.52 (s, Cp, 5H), 7.38–8.15 (m, aromatic, PPh₃, 15 H). ¹³C{¹H} NMR (acetone-*d*₆): δ 43.55 (d, ¹J_{CP} = 20.0 Hz, PCH₂N), 53.43 (s, CH₃), 55.35 (d, ¹J_{CP} = 37.20 Hz, PCH₂NCH₃), 77.27 (s, CH₃NCH₂NCH₃), 78.72 (s, NCH₂NCH₃), 119.63 (q, ¹J_{CF} = 318.00 Hz, OTf), 127.89–138.45 (m, aromatic, PPh₃). ³¹P{¹H} NMR (acetone-*d*₆): δ -6.34 (d, ²J_{PP} = 41.66 Hz, dmPTA), 44.32 (d, ²J_{PP} = 41.66 Hz, PPh₃).

Reactivity of 3 with [RuClCp(PPh₃)₂] in Acetone-*d*₆ and H₂O. In a manner similar to that described previously, a 5 mm NMR tube was charged with **3** (6 mg, 0.03 mmol), [RuClCp(PPh₃)₂] (25 mg, 0.03 mmol), 0.5 mL of acetone-*d*₆, and 10 μL of H₂O. The solution was kept at 50 °C and analyzed every 10 min by NMR. The main signals obtained after 12 h were the same as those

Scheme 1



Scheme 2

**Table 1.** Crystal Data and Data Collection Details for **1** and **4**

	1	4
formula	C ₁₀ H ₂₀ N ₃ F ₆ O ₇ P ₁ S ₂	C ₃₂ H ₄₁ N ₃ F ₃ ClO ₄ P ₂ RuS
fw	503.36	819.18
cryst syst	orthorhombic	triclinic
space group	<i>Pnma</i>	<i>P1</i>
<i>a</i> (Å)	18.833(4)	9.162(5)
<i>b</i> (Å)	8.9106(18)	14.336(5)
<i>c</i> (Å)	11.965(2)	15.123(5)
α (deg)	90.00	77.226(5)
β (deg)	90.00	74.345(5)
γ (deg)	90.00	77.086(5)
<i>V</i> (Å ³)	2007.9(7)	1836.7(13)
<i>Z</i>	1	2
<i>d</i> _{calcd.} (g·cm ⁻³)	1.711	1.509
abs coeff (mm ⁻¹)	0.444	0.700
wavelength (Å)	0.71073	0.71073
data/restraints/params	2605/0/155	5226/0/452
final R indices	R1 = 0.0604	R1 = 0.0911
[<i>I</i> > 2σ(<i>I</i>)]	wR2 = 0.1537	wR2 = 0.1737
R indices	R1 = 0.0864	R1 = 0.0517
(all data)	wR2 = 0.1819	wR2 = 0.1163
largest diff	0.668	0.640
peak and hole (e Å ³)	-0.501	-0.781

obtained for **4** (80%), but other signals were also present which could not be characterized.

X-ray Structure Determinations. A crystal of compound **1** and **4** was mounted on a glass fiber with epoxy cement at room temperature. Crystal data and data collection details are given in Table 1. Data collection for **1** was performed on a KappaCCD diffractometer (XDIFRACT service of the University of La Laguna) in the range of $2.02 \leq 2\theta \leq 28.63$. Lorentz and polarization corrections were applied to 16 741 reflections collected, of which 2049 were unique with $I_0 > 2\sigma(I_0)$. For **4**, data collection was performed on a Bruker APEX CCD diffractometer (XDIFRACT service of the University of Almería) in the range of $1.42 \leq 2\theta \leq 23.27$. The usual corrections were applied to 8560 reflections, of which 3195 were unique with $I_0 > 2\sigma(I_0)$.

Both structures were determined by direct methods (SIR97¹⁶ or SHELXS-XTL)¹⁷ and refined by least-squares procedures on *F*²

(SHELX-XTL). The function minimized during the refinement was $w = 1/[\sigma^2(F_0^2) + (0.0742P)^2 + 1.6850P]$ for **1** and $w = 1/[\sigma^2(F_0^2) + (0.0737P)^2 + 0.0000P]$ for **4**, where $P = [(\max(F_0^2) + 2F_c^2)/3]$. The final geometrical calculations and the graphical manipulations were carried out with the SHELXS-XTL package.¹⁷

Results and Discussions

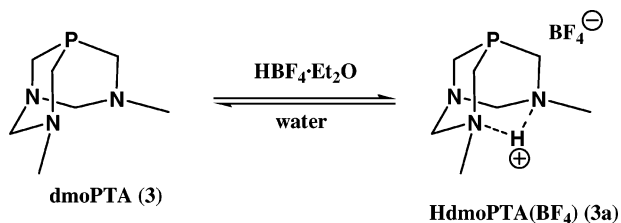
The growing interest in obtaining new water-soluble phosphine ligands led us to synthesize the *N,N*-dimethyl derivative of PTA that was accomplished by reaction of PTA with 2 equiv of Me(CF₃SO₃) in refluxing acetone (Scheme 1). The white powder obtained was soluble in organic solvents and water, in which it was characterized by NMR, IR spectroscopy, and elemental analysis.

The ¹H NMR spectrum was assigned by using 2D-¹H COSY and ¹H{³¹P} NMR. The spectrum displays a singlet at 3.16 ppm (6 H) in D₂O that is in agreement with the double methylation on two N atoms of PTA. The observed chemical shift for NCH₃ in **1** is shifted 0.49 ppm to low field from the NCH₃ signal in mPTA(CF₃SO₃) (2.67 ppm).¹¹ The PCH₂N appears as a broad doublet at 3.85 ppm by coupling with the P atom, while the two equivalent PCH₂NCH₃ groups arise as a multiplet from 4.27 to 4.63 ppm. The two NCH₂-NCH₃ protons are together with CH₃NCH₂NCH₃ protons in the range of 4.92–5.21 ppm. It was not possible to obtain the ¹³C{¹H} NMR of **1** in D₂O because this solvent transforms it slowly into dmoPTA (**3**). In DMSO-*d*₆ and acetone-*d*₆, the observed carbon chemical shifts are similar, the largest difference being for NCH₃ (52.12 ppm in DMSO-*d*₆ and 51.65 ppm in acetone-*d*₆) which is, in addition, the

(16) Altamore, A.; Cascarano, G.; Giacobozzo, C.; Guagliardi, A.; Moliterni, G.; Burla, M. C.; Polidori, G.; Camalli, M.; Spagna, R. *Sir 97 Package Program*; Institute of Crystallography: Trieste, Italy, 1997.

(17) Sheldrick, G. M. *SHELXTL*, version 6.14; Bruker-AXS: Madison, WI, 2003.

Scheme 3



only signal shifted to field lower than that for mPTA (49.92 ppm in D_2O). A quartet that only could be ascribable to $^-\text{OSO}_2\text{CF}_3$ arises at 120.78 ppm (acetone- d_6). Finally, the $^{31}\text{P}\{^1\text{H}\}$ NMR for **1** in D_2O is composed of a singlet signal at -80.78 ppm, ~ 5 ppm to field lower than that for mPTA (-85.10 ppm). The proposed structure for **1** was confirmed by X-ray monocrystal diffraction of white crystals obtained by slow evaporation of its acetone solution.

Reaction of **1** with 2 equiv of NaBF_4 in acetone led to the synthesis of $\text{dmPTA(BF}_4\text{)}_2$ (**2**) which precipitated as a white powder. Easy substitution of $^-\text{OSO}_2\text{CF}_3$ by BF_4^- confirmed that there are not important interactions between the dication dmPTA and the anion $^-\text{OSO}_2\text{CF}_3$ in solution (Scheme 1). All spectroscopic features for **2** are similar to those of **1**, except for those attributable to the anion.

As a general target, we are interested in obtaining new water-soluble Cp–ruthenium complexes because they could mediate catalytic reactions in an aqueous medium, as well as being active against biomolecules.¹¹ The strategy used to obtain such complexes involves the substitution of one or both PPh_3 ligands from $[\text{RuClCp(PPh}_3\text{)}_2]$ by water-soluble phosphines. The reaction of **1** with $[\text{RuClCp(PPh}_3\text{)}_2]$ in refluxing acetone, using this general procedure, gave a yellow powder which was crystallized in methanol. Yellow crystals for $[\text{RuClCp(HdmoPTA)(PPh}_3\text{)}](\text{OSO}_2\text{CF}_3)$ (**4**) were separated from the solution and characterized by spectroscopic techniques and X-ray monocrystal diffraction. Its ^1H NMR displays a singlet at 4.55 ppm, which is characteristic of a $^5\eta\text{-Cp}$ bonded to a Ru, and signals ascribable to PPh_3 (15 H). The rest of the signals observed must be assigned to the dmPTA ligand, but their integration was 10 H instead of 12 H as expected. A contrasting analysis between the ^1H NMR spectra of **1** and **4** suggests that the lost group is the methylene bonded to both quaternary nitrogen atoms ($\text{CH}_3\text{NCH}_2\text{NCH}_3$). That suspicion was confirmed by the $^{13}\text{C}\{^1\text{H}\}$ NMR of **4** because the signals for Cp, PPh_3 , and most of the carbons for dmPTA were assigned, but there was no signal observed for the $-\text{CH}_2-$ between the NCH_3 groups. Therefore, the NMR features suggest that complex **4** contains a new ligand which formed from the elimination of the $-\text{CH}_2-$ group present in the starting ligand dmPTA. The $^{31}\text{P}\{^1\text{H}\}$ NMR in CD_3OD showed two doublets at 46.00 and -2.93 ppm that only could be assigned to coordinated PPh_3 and a new phosphine derived from PTA, respectively.

The X-ray structure showed that complex **4** is constituted by a ruthenium bonded to a $^5\eta\text{-Cp}$, a Cl, a PPh_3 , and a new ligand (HdmoPTA) produced from dmPTA by elimination of the $-\text{CH}_2-$ group between CH_3N atoms (vide infra). The complex is positively charged because one H^+ is located

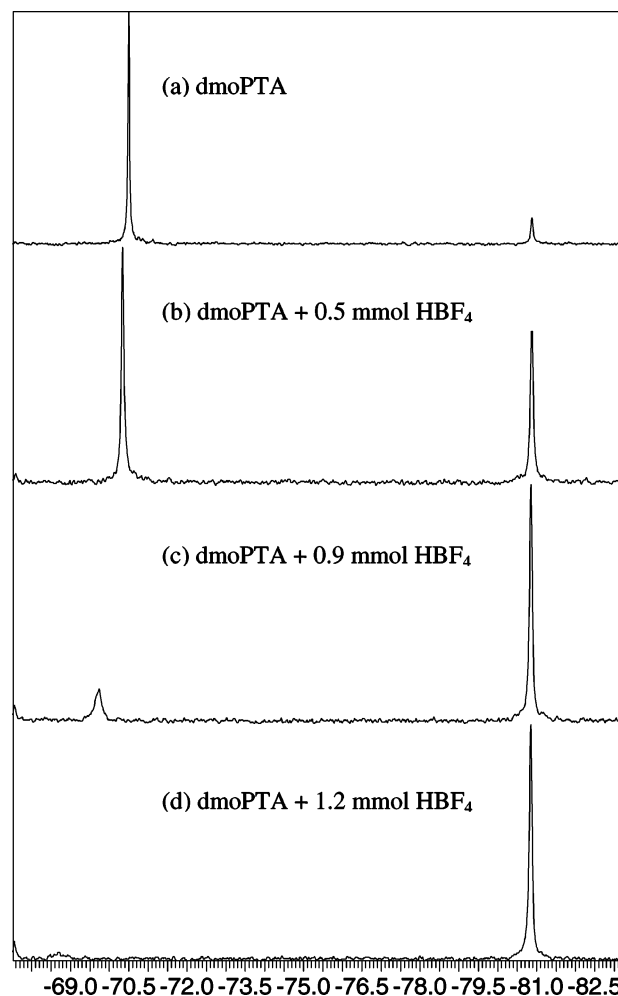


Figure 1. $^{31}\text{P}\{^1\text{H}\}$ NMR spectra in D_2O of **3** (a) and **3** + $\text{HBF}_4 \cdot \text{Et}_2\text{O}$ (0.5 mmol (b), 0.9 mmol (c), 1.2 mmol (d)).

between both CH_3N units with a $^-\text{OSO}_2\text{CF}_3$ counterion. This proton was able to be located in a subsequent difference Fourier syntheses.

Compound **1** was spectroscopically studied under various conditions to determine if coordination of the ligand to the metal was required for the elimination of the $-\text{CH}_2-$ group. When **1** was reacted with 1 equiv of $\text{HBF}_4 \cdot \text{Et}_2\text{O}$ in D_2O , **2** was the only compound observed. However, when the reaction was performed with KOH, a new compound was obtained that was stable enough in water to be characterized by NMR. Evaporation of the solvent afforded a white powder. The $^{31}\text{P}\{^1\text{H}\}$ NMR spectrum of the powder in D_2O was identical to that obtained before evaporation, thus indicating that the same P-containing species was present. The ^1H NMR spectra before and after the evaporation were different in that a singlet at 4.72 ppm was lost upon removal of the solvent. This indicated that a molecule was removed upon evaporation. This hypothesis was supported by the $^{13}\text{C}\{^1\text{H}\}$ NMR. Removal of the solvent caused a singlet at 81.76 ppm to be lost. Both missing signals are in agreement with those expected for $\text{CH}_2(\text{OH})_2$, and therefore that could be the resulting compound in which the $-\text{CH}_2-$ group between CH_3N atoms is transformed. That suspicion was supported by addition of CH_2O into the solution as missing signals in

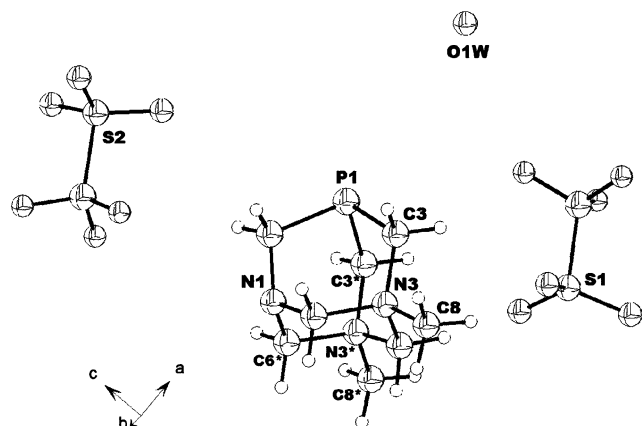


Figure 2. ORTEP diagram of dmPTA(OSO₂CF₃)₂ H₂O (**1**) with atom numbering scheme showing 50% probability thermal ellipsoids (* indicates atoms at equivalent positions: $x, 1/2 - y, z$).

¹H and ¹³C NMR were newly observed. Formaldehyde is only possible to be generated from this reaction if an OH⁻ anion attacks onto -CH₂- carbon atom between quaternary nitrogen atoms (Scheme 2). There are two possible processes: (a) a unique OH⁻ is involved to generate the dmoPTA molecule and H₂CO, which by reaction with H₂O provides the observed H₂C(OH)₂ (Scheme 2a); (b) two OH⁻ are implicated in the reaction which gives rise to the dmPTA ligand and H₂C(OH)₂ (Scheme 2b).

Reaction of **1** with 0.8 equiv of KOH in a NMR tube provided dmoPTA in an 80% yield which suggested that the first proposed possible process (Scheme 2a) is the most probable. Nevertheless, to determine the real mechanism further studies have to be performed.

Preparative synthesis of dmoPTA (**3**) was accomplished by reaction with KOH in water and MeOH. The yield for the synthesis of **3** in water was the best, but the practical procedure is more complicated and longer than in MeOH. The **3** ¹H NMR is similar to that for dmPTA, but the integration shows that 2 protons are lost. The multiplet between 3.96 and 4.28 ppm, which was assigned in dmPTA to the NCH₂N groups, integrates by 4 H instead of expected 6 H. Signals for the rest of the protons were found but at a field somewhat higher than those for dmPTA protons. As expected, the signal for NCH₃ is the most shifted, arising in dmoPTA at 2.37 ppm but in dmPTA at 3.26 ppm. The ¹³C-{¹H} NMR provided the definitive support that -CH₂- was eliminated because no signal at ~77 ppm was observed. Rest of signals for new phosphine were assigned, which arose at

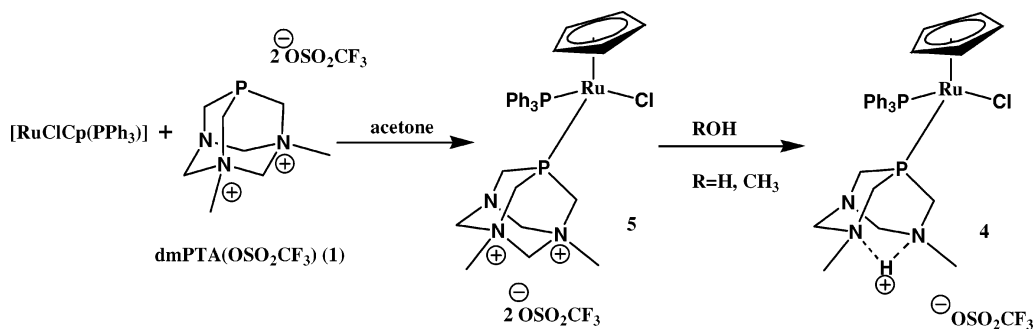
a similar chemical shift to that for dmPTA, the biggest chemical shift difference being for the CH₃N carbon (dmPTA, 51.65 ppm; dmoPTA, 43.02 ppm). The ³¹P{¹H} NMR for **3** was constituted by a singlet at -70.72 ppm, 10 ppm shifted toward low field than that for dmPTA.

Ligand dmoPTA is able to be protonated in water by 1 equiv of HBF₄·Et₂O to give stoichiometrically a new compound which was not enough stable in water to be characterized by ¹³C{¹H} NMR and be isolated. Its ³¹P and ¹H NMR suggest that the new compound is a consequence of the incorporation of a proton between both N atoms of the dmoPTA bonded to -CH₃ that gives rise to a new ligand, the HdmoPTA (Scheme 3). It is interesting to point out that protonation rate depends on the acid equivalents added to the reaction (Figure 1).

The addition of 1 equiv of KOH to the water solution of HdmoPTA(BF₄) brought about the ligand dmoPTA (Scheme 3). It is important to point out that unfortunately the ligand HdmoPTA is unstable in water at room temperature, decomposing in 15 min to produce a mixture of compounds that were not possible to characterize. Protonation in other solvents (CD₃OD, acetone-*d*₆) led to results similar to those obtained in water, but in these solvents, ligand HdmoPTA was a little more stable. In acetone-*d*₆, it was not possible to observe the N···H···N atom which suggests that this proton moves between both N atoms. It is important to point out that the -NCH₃ chemical shift for HdmoPTA arose as a unique singlet at 3.58 ppm which is a characteristic chemical shift for protonated tertiary amines, close to that observed for **1** (3.16 ppm) but far from that for **3** (2.37 ppm). The chemical shift of the singlet for CH₃N supports the idea that a H⁺ has to be located between the two CH₃N atoms. Unfortunately **3a** was not able to be isolated and characterized by other spectroscopic techniques which would be able to support that suspicion.

Reaction of [RuClCp(PPh₃)₂] with ligand dmoPTA in acetone led to **4** but in yields lower than that found for the previously described reaction with dmPTA. The in situ reaction between dmoPTA and [RuClCp(PPh₃)₂] in acetone-*d*₆ showed that the compound in the greatest amount was **4** but that other compounds are also present, the identities of which were not determined. By a similar experiment, the reaction between dmPTA and [RuClCp(PPh₃)₂] provided products depending on the solvent used: dry acetone-*d*₆, acetone-*d*₆ and traces of H₂O, acetone-*d*₆ and traces of CH₃-

Scheme 4



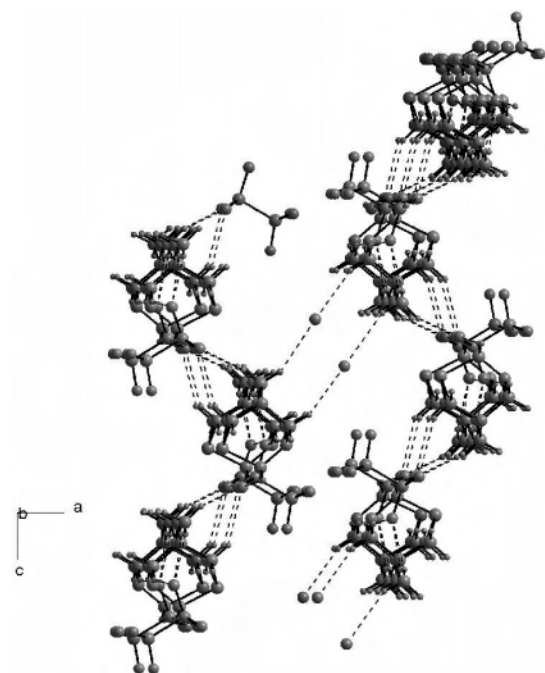


Figure 3. Spatial distribution of dmPTA(OSO₂CF₃)₂ H₂O (**1**) showing the hydrogen-bonding C_{dmPTA}-H···O_{Tf} and C_{dmPTA}-H···O_w.

Table 2. Selected Bond Lengths (Å) and Angles (deg) for **1** and **4**

compound 1			
P1–C1	1.832(6)	N3–C3	1.515(4)
P2–C3	1.829(3)	N3–C5	1.507(3)
N1–C1	1.466(7)	N3–C6	1.554(4)
N1–C6	1.424(4)	N3–C8	1.499(4)
C1–P1–C3	97.24(15)	C3–N3–C6	110.3(2)
C3–P1–C3	96.6(2)	N3–C5–N3 ^a	111.9(3)
N1–C1–P	112.8(3)	N1–C6 ^a –N3 ^a	110.8(2)
compound 4			
Ru1–C _{av}	2.221(9) ^b	C6P–N1P	1.488(11)
Ru1–P1	2.291(3)	C2P–N2P	1.461(11)
Ru1–P2	2.277(3)	C4P–N2P	1.429(12)
Ru1–C11	2.447(2)	C5P–N2P	1.419(11)
P1–C _{av}	1.840(9) ^c	C1P–N3P	1.457(11)
P2–C _{av}	1.844(9) ^c	C4P–N3P	1.453(12)
C3P–N1P	1.478(10)	C7P–N3P	1.446(12)
C5P–N1P	1.527(11)		
P1–Ru1–P2	98.38(9)	P2–Ru1–C11	88.42(9)
P1–Ru1–C11	90.89(9)		

^a Atoms equivalent positions: $x, 1/2 - y, z$. ^b Average of five values. ^c Average of three values.

OD. The ³¹P{¹H} NMR showed that in dry acetone-*d*₆ the main compound obtained, which is not **4**, was characterized by a doublet of doublets at –6.34 and 44.32 ppm, which is characteristic of a compound containing PPh₃ and PTA derivatives bonded to the metal. The analysis of the ¹H NMR and ¹³C{¹H} NMR showed the presence of the expected signals for the CH₃NCH₂NCH₃ methylene group, and no signals for CH₂O were observed. Therefore, it is reasonable to suppose that this new compound is [RuClCp(PPh₃)(dmPTA)] (**5**) which results from the substitution of a PPh₃ by a dmPTA ligand in the starting complex [RuClCp(PPh₃)₂] (Scheme 4). This complex was stable for 24 h in solution at room temperature. Unfortunately, it was not possible to isolate the complex. Compound **5** was slowly converted into **4** by the addition of H₂O. If the reaction between dmPTA

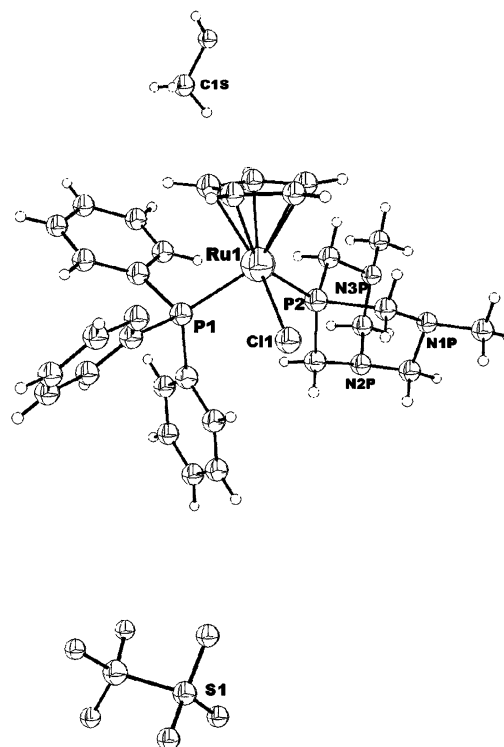


Figure 4. ORTEP diagram of [RuClCp(PPh₃)(HbmoPTA)(OSO₂CF₃)CH₃OH (**4**) with atom numbering scheme showing 50% probability thermal ellipsoids.

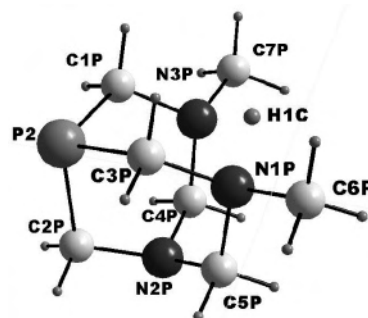


Figure 5. Cation unit HdmPTA⁺.

and [RuClCp(PPh₃)₂] was performed in wet acetone the same conversions were observed. The rate of the transformation of **5** into **4** depended on the amount of water in the reaction; the largest amount of water provided fastest reaction. Other minor phosphorus-containing compounds were also observed, but they could not be characterized. When the transformation of **5** into **4** was examined in CH₃OH, similar results were observed; however, the conversion rate was slower.

The results obtained from this reaction suggest that the CH₃NCH₂NCH₃ methylene group was removed after the substitution of one PPh₃ in the starting ruthenium complex by a dmPTA molecule (Scheme 4). Therefore, the rate of the –CH₂– elimination is slower than that of the substitution reaction.

Crystal Structure of dmPTA(OSO₂CF₃)₂ H₂O (1**).** Single-crystal X-ray crystallography of dmPTA (**1**) showed that the structure consists of well-separated molecular units. Compound **1** crystallized in the orthorhombic space group *Pnma* (Table 1) and the thermal ellipsoid drawing is shown

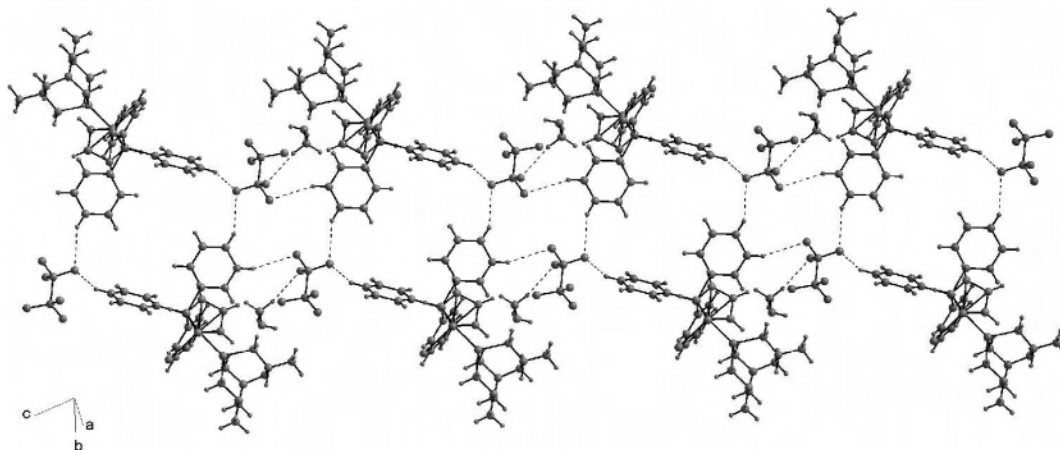


Figure 6. Packing diagram (section) of **4** highlighting the intermolecular interactions between hydrogen atoms of $C_{PPh_3}-H \cdots FOSO_2CF_3$ and $C_{MeOH}-H \cdots FOSO_2CF_3$.

in Figure 2. Selected bond distances and bond angles are listed in Table 2. Previous works^{6,12,13,15} have proven that the (N)C–N bond lengths are the most affected after protonation and alkylation of PTA nitrogen atoms. Carbon–nitrogen bond distances corresponding to the nitrogen-supporting methyl group (N3/N3*) are between 1.507(3)–1.554(4) Å (see Table 2). Carbon–nitrogen bond distances corresponding to the nonsubstituted nitrogen atom (N1) are close to those observed for PTA (average C–N_{PTA} bond length = 1.463(4) Å).¹⁵ The dmPTA P–C bond distances are similar enough to the adamantyl structure (1.840(5) Å).¹⁵ The angle $\angle C(3)-P(1)-C(3^*)$ is calculated to be 96.6(2)°, while the remaining angle $\angle C(1)-P(1)-C(3)$ is 97.24(15)°, consistent with the corresponding C–P–C bond angle in PTA (i.e., 96.1(1)–98.03(9)°).¹⁵

The crystal structure includes a molecule of water, which is held in place by hydrogen bonding to a dmPTA carbon atom belonging to two different 2D chains in the *a*-direction (Figure 3).

Crystal Structure of [RuClCp(PPh₃)(HdmPTA)](CF₃SO₃) CH₃OH (4**).** Details of the metal coordination environment in complex **4** were revealed from a single-crystal X-ray structure determination of monocrystal samples obtained from a MeOH solution. The space group for crystal cell is $P\bar{1}$ (Table 1). The crystal structure, including the thermal ellipsoid representation of **4**, is depicted in Figure 4, together with the atomic labeling system. Selected bond distances and bond angles are listed in Table 2.

Comparison of the structure for **4** with the parent complex [RuClCp(PPh₃)(PTA)]¹¹ reveals that the core organometallic portion of **4** is largely unchanged. The P1–Ru1–P2 angle is slightly less obtuse ($\sim 0.6^\circ$), whereas the Ru–P bond distances are elongated slightly (~ 0.005 Å) in **4** versus complex [RuClCp(PPh₃)(PTA)].¹¹ The carbon–nitrogen bond distances corresponding to the nitrogen atom adjacent (N1P or N3P, Figure 4) to the methyl group are in the range of 1.453(12)–1.527(11) Å (see Table 2). The carbon–nitrogen bond distances corresponding to the nonsubstituted nitrogen atom (N2P) are consistent with those found in known PTA complexes, in which one nitrogen atom of PTA has not been protonated or alkylated (vide supra). Other bond distances

and angles show no particular features in addition to the contact distances.^{6,11}

Another important characteristic of the complex is the proton site (Scheme 4), considering a sharing-situation with the hydrogen located just between the nitrogen atoms N1P and N3P (Figure 5). The sort intramolecular contact (N1P \cdots N3P = 2.702(1) Å) can support this hypothesis, with a solid-state packing stabilized by a hydrogen-bond interaction. On the other hand, the difference between the N1P–C6P and N3P–C7P bond distances is ~ 0.042 Å, that is, probably caused by delocalization of the H⁺ bond¹⁸ which occurs when the proton is lost and the bridge is formed (N3P \cdots H1C \cdots N1P = 116.8(2)°). Finally, the torsion angles show that the cationic unit HdmPTA⁺ is not symmetric as shown by torsion angles (C5P–N1P–C5–P2 = 54.5°, C4P–N3P–C1P–P2 = 58.9°) and distances from the atoms C7P, N3P, N1P, and C6P to plane “C2P–P2–C1P” (1.01, 1.02, 2.73, and 4.13 Å, respectively).

A 3D network through extensive hydrogen bonding involving PPh₃, MeOH, and CF₃SO₃[−] (Figure 6) forms the crystal structure.

Conclusions

The new water-soluble ligands dmPTA(CF₃SO₃) (**1**) (dmPTA = *N,N'*-dimethyl-1,3,5-triaza-7-phosphaadamantane), dmoPTA (**3**) (dmoPTA = 3,7-dimethyl-1,3,7-triaza-5-phosphabicyclo[3.3.1]nonane), and complex [RuClCp(HdmPTA)(PPh₃)](CF₃SO₃) (**4**) have been obtained. Additionally, ligand HdmPTA (**3a**) and complex [RuClCp(dmPTA)(PPh₃)] (**5**) have been characterized. Ligand **3** was obtained by removal of the CH₃NCH₂NCH₃ methylene group from **1** by reaction with KOH. In the synthesis of **4**, the dmPTA ligand substituted a PPh₃ from the starting ruthenium complex [RuClCp(PPh₃)₂], and the CH₃NCH₂NCH₃ methylene group was removed afterward. Therefore, the CH₂ elimination is slower than the substitution reaction. Finally, it was not necessary to include KOH, but instead,

(18) (a) Berthold, H. J.; Preibsch, W.; Vonholdt, E. *Angew. Chem., Int. Ed. Engl.* **1988**, *27*, 1524. (b) Daly, J. J.; Wheatley, P. J. *J. Chem. Soc. A* **1967**, 212.

enough H₂O (or CH₃OH) was needed to eliminate the methylene group between quaternary N atoms from **5** dmPTA; therefore, the previous coordination to {RuClCp-(PPh₃)} of dmPTA favors the elimination of its CH₃NCH₂-NCH₃ methylene group.

Acknowledgment. Funding for this work is provided by Junta de Andalucía through PAI (research team FQM-317) and project AM55/04, the MCRTN program AQUACHEM (MRTN-CT-2003-503864), the COST Actions D17 and D29, and the MCYT (Spain) project CTQ2006-06552/BQU. We also thank the Consejería de Educación, Cultura y Deportes

(Gobierno Autónomo de Canarias, Spain) for support to A.M.C. We acknowledge the assistance of the Dr. Platas, J.G. (XDIFRACT service of the University of La Laguna) for RX analysis.

Supporting Information Available: Crystallographic data of the structures **1** and **4** in CIF format. This material is available free of charge via the Internet at <http://pubs.acs.org>. Data for **1** and **4** are deposited with the Cambridge Crystallographic Data Centre (www.ccdc.cam.ac.uk) under CCDC 635227 and 635228, respectively.

IC070168M